Light Metals 2012 *Edited by: Carlos E. Suarez*
TMS (The Minerals, Metals & Materials Society), 2012

THERMAL ANALYSIS AND MICROSTRUCTURES OF MODIFIED GRAIN-REFINED Al-7Si-Mg CAST ALLOY

A.M.A. Mohamed, [1,2] F.H. Samuel,[1,3] Saleh Alkahtani[4]

[1]Université du Québec à Chicoutimi, Chicoutimi, Québec, Canada, G7H 2B1
[2]Department of Metallurgical and Materials Engineering, Faculty of Petroleum and Mining Engineering, Suez Canal University, Box 43721, Suez, Egypt, madel@uqac.ca
[3]Center of Excellence for Research in Engineering Materials, College of Engineering, King Saud University, Riyadh, Saudi Arabia
[4]Industrial Engineering Program, Mechanical Engineering Department, College of Engineering, Salman Bin Abdulaziz University, AlKharj, Saudi Arabia

Keywords: Al-Si-Mg Alloys, Grain Refining, Modification, Thermal Analysis, Metallography.

Abstract

This article aims to investigate the grain refining response of Sr-modified A356.2 alloy with various Al-Ti, Al-B and Al-Ti-B master alloys at different levels. Thermal analysis was used to evaluate the interactions between Sr and B, and between Sr and Ti. Microstructure was examined using optical microscopy and EPMA technique. Impact properties were evaluated for both as-cast and heat-treated conditions. The results reveal that adding B with levels higher than 0.1% leads to formation of particles containing predominantly B and Sr, such as SrB_6. The Sr-B interaction may postpone grain refinement of the alloy containing 0.02-0.1%B. It is also observed that the Al-Ti-B and Al-4%B types of master alloy have a greater influence on the grain refining of the A356.2 alloy than does Al-10%Ti. The grain size of the alloy decreases rapidly with an increase in boron-content for the lower levels of boron addition.

Introduction

Aluminum-Silicon (Al-Si) alloys constitute an important class of alloys used in aluminum foundries, in large part because of their excellent casting characteristics. The properties displayed by these alloys make them popular for the various applications required by such fields as the automotive, aerospace and defence industries. With the addition of certain elements to Al-Si alloys, a wide range of physical and mechanical properties may be obtained, including high corrosion resistance, good weldability, low shrinkage, low thermal expansion and high tensile properties. Magnesium and copper are two of the most important alloying additions, so that within Al-Si alloys, Al-Si-Mg, Al-Si-Cu and Al-Si-Cu-Mg are the three main alloying systems, for which A356, A319 and B319 alloys are typical examples.

With regard to grain refining in hypoeutectic Al-Si alloys, it is taken as a matter of course that the α-Al is refined by the addition of a grain refiner. A fine equiaxed grain structure then results in a number of benefits including high yield strength, greater toughness values, and improved machinability [1-3]. Grain refiners are generally added in the form of master alloys of the type Al-Ti, Al-Ti-B or Al-B [4-6]. Aluminum-Titanium-Boron master alloys, such as Al-5Ti-1B contain two active intermetallic phases, namely, Al_3Ti and TiB_2, while Al-Ti types contain Al_3Ti particles only. The TiB_2 and Al_3Ti particles provide heterogeneous nucleation sites for α-Al during solidification, at which time TiB_2 particles show evidence of a stronger effect than do the Al_3Ti particles [7]. Sigworth and Guzowski [8] also reported that, when using an Al-4%B master alloy, it is possible to obtain satisfactory grain refinement in the A356.2 alloy, which is even better than that obtained using the Al-5Ti-1B master alloy.

According to Johnsson [9], Al_3Ti particles in master alloys usually appear in block form with particle sizes between 5 to 15 µm, some of which may even go as high as 50 µm. The size of the Al_3Ti particles and the value of the target concentration are of considerable importance since they determine the time required for full dissolution. Lee *et al.* [10] reported that the TiB_2 particles are rendered less potent in Al–Si foundry alloys due to the formation of such Ti-Si compounds as Ti_5Si_3, on the surface of TiB_2 particles in the presence of high Si in the melts. When both Ti and B are available in molten aluminium, the percentage of Ti determines the solubility of the boron. Thus, if this percentage is reduced, the solubility of boron increases correspondingly. Boron does not reduce the Al_3Ti dissolution rate by reducing the solubility of Ti; instead, the dissolution rate of Al_3Ti determines the dissolution rate of TiB_2.

In the A356 alloy, individual additions of the grain refiner raise the primary α-Al nucleation temperature by as much as 4-5°C, while additions solely of the Sr-modifier will depress the eutectic temperature by almost 7-8°C. In other words, if both additives perform in the same manner when combined, the solidification range, or the temperature difference from the α-Al nucleation temperature to the eutectic temperature, should increase by 11-13°C [11]. It was reported that the addition of Sr to Al-11.6%Si alloys promotes the columnar growth of primary Al dendrites, a condition which is deleterious to the mechanical properties of alloys. Thus, subsequent grain refinement of primary Al dendrites becomes a necessary step to further materialize the beneficial effects of eutectic modification on the properties. They also reported that Sr addition affects the amount of dendritic α-Al phase [12, 13].

The present study aims at investigating the influence of the addition of Ti and B in the form of five different grain refiners/aluminium master alloys (Al-10%Ti, Al-5%Ti-1%B, Al-2.5%Ti-2.5%B, Al-1.7%Ti-1.4%%B and Al-4%B) in conjunction with that of Sr (as modifier) added in the form of Al-10%Sr master alloy to A356.2 alloy. The occurrence of any probable Sr-Ti and/or Sr-B interactions was investigated using electron microprobe analysis and metallographic techniques. Thermal analysis was also used to examine the combined interaction between strontium and boron, as well as the likely effect of boron on the partial modification of the eutectic Si particles, through a study of the cooling curves obtained upon solidification of the corresponding melts.

Experimental Procedure

The A356.2 alloy was received in the form of 12.5 kg-ingots. Table 1 lists the chemical composition of the alloy studied. The ingots were first cut into smaller pieces, then cleaned, dried and melted in a 40-kg capacity SiC crucible using an electrical resistance furnace. The molten metal was maintained at a temperature of 750 ± 5°C. Addition of 200 ppm Sr was made using Al-10%Sr master alloy. Grain-refiner additions were then made to the Sr-modified alloy melts in various concentrations and using different types of grain refiner in the form of master alloys, such as Al-10% Ti, Al-4% B, Al-5%Ti-1%B, Al-2.5%Ti-2.5%B, and Al-1.7%Ti-1.4%B. The melt was stirred, and then degassed for 15 minutes using pure, dry argon introduced into the melt through a graphite rotary impeller operating at a speed of 150 rpm. Following degassing, the melt was poured at 735 ± 5°C into coated metallic molds preheated at 440 ± 10°C.

Table 1. Composition (wt %) of the A356.2 alloy

Si	Mg	Cu	Ti	Mn	Zn	Fe	Al
7.21	0.41	< 0.01	0.11	< 0.01	< 0.01	0.08	Bal.

Thermal analysis was performed by attaching a high sensitivity thermocouple (chromel-alumel, type K) to the mold system, passing through the bottom of the mold and reaching halfway up into the mold cavity. The parts of the thermocouple within the mold were protected using double-walled ceramic tubing. The temperature-time data was collected using a high-speed data acquisition system linked to a computer with an acquisition rate of 5 readings/sec. From the thermal analysis data, the cooling curves were plotted in each case.

The metallographic samples were examined using optical microscopy and electron probe microanalysis (EPMA) associated with energy dispersive X-ray (EDX) and wavelength dispersion spectroscopic (WDS) analyses. The grain sizes of the specimens were measured by the linear intercept method after etching the polished surface with Keller's reagent.

Results and Discussion

Characterization of Macrostructures and Microstructures

Figure 1 shows the macrostructures of 200 ppm Sr-modified A356.2 alloy refined with Al-10%Ti and Al-4%B master alloys. It is clear from Figure 1(a) that, in the absence of an addition of grain refiner, the A356.2 alloy shows columnar grains at the periphery and equiaxed grain at the center. However, with an increase in the addition level of grain refiner, the grain structure of the alloy becomes finer for each subsequent addition level, as shown in Figures 1(b) to (e). Satisfactory grain refinement, *i.e.* a fine equiaxed grain structure was obtained in this alloy by the addition of 0.05% B using Al-4%B; this is supported by the fact that numerous fine TiB_2 particles were formed.

The influence of three different Al-Ti-B master alloys on 200 ppm Sr-modified A356.2 alloy is illustrated in Figures 2(a) through (f). A large number of the fine TiB_2 particles will ultimately be transformed into heterogeneous nucleation sites for liquid aluminum, as will the excess titanium atoms occurring in the form of Al_3Ti. Grain size is sufficiently fine at the high addition rates for all boron-bearing master alloys as is made abundantly clear in Figure 2.

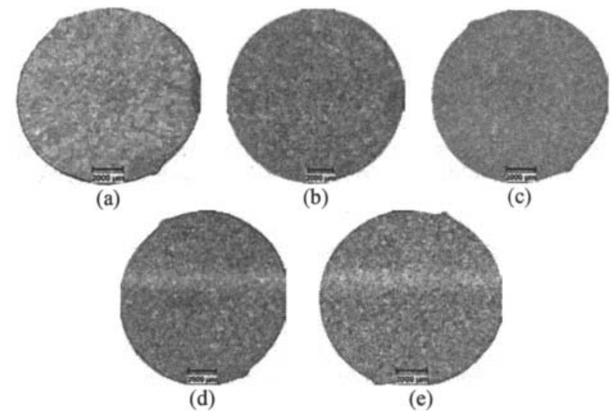

Figure 1. Macrostructures of (a) A356.2 alloy without any grain refiner addition, and (b-e) 200 ppm Sr-modified A356.2 alloy refined with (b, c) 0.1% Ti and 0.5% Ti, using Al-10%Ti; and (d, e) 0.01% B and 0.05% B, using Al-4%B.

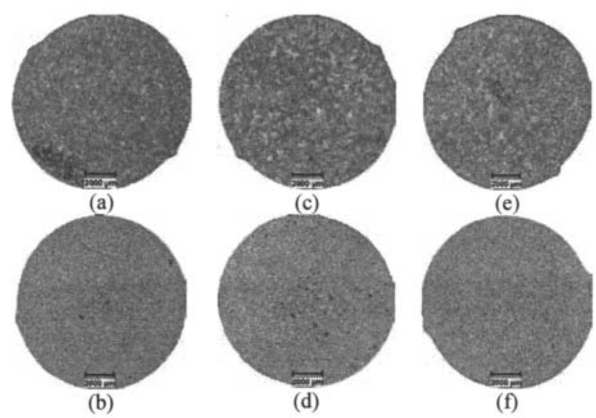

Figure 2. Macrostructures of 200 ppm Sr-modified A356.2 alloy refined with: (a, b) 0.1% and 0.5% Ti, using Al-5%Ti-1%B; (c, d) 0.1% and 0.5% Ti, using Al-2.5%Ti-2.5%B; and (e, f) 0.1% and 0.5% Ti, using Al-1.7%Ti-1.4%B master alloys, respectively.

The grain size values of Sr-modified A356.2 alloy with addition of different grain refiners are shown in Figure 3. It may be observed that the Al-Ti-B and Al-4%B types of master alloy have a greater influence on the grain refining of the A356.2 alloy than does Al-10%Ti. It is evident that the grain size of alloy decreases rapidly with an increase in boron-content for the lower levels of boron addition. As regards the Al-5%Ti-1%B master alloy, significant refining is achieved with the sole addition of 0.02% Ti (or 0.004% B), yet no further refining occurs with increasing additions of up to 0.1% Ti (or 0.02% B), and with an addition of 0.5% Ti (or 0.1% B) a further drop in grain size may be observed. An interesting point emerges in connection with the master alloys Al-2.5%Ti-2.5%B and Al-1.7%Ti-1.4%B when the addition level shifts from 0.08% to

0.1% B. Measurements indicate a certain amount of coarsening, or deterioration in the grain-refining effect, when the abovementioned range of boron additions is made to the Sr-modified alloy using these two master alloys. The adverse effect of the Sr-B interaction may be considered for justifying this coarsening. It is interesting to note that this coarsening is not evident in the case of Al-5%Ti-1%B compared to the other Al-Ti-B master alloys, as shown in Figure 3. This figure also shows that when the boron content is further increased to over 0.1% B, the refining recommences, which may be attributed to the increased number of TiB_2 and Al_3Ti particles made available due to the higher addition, thereby restoring the grain-refining effect.

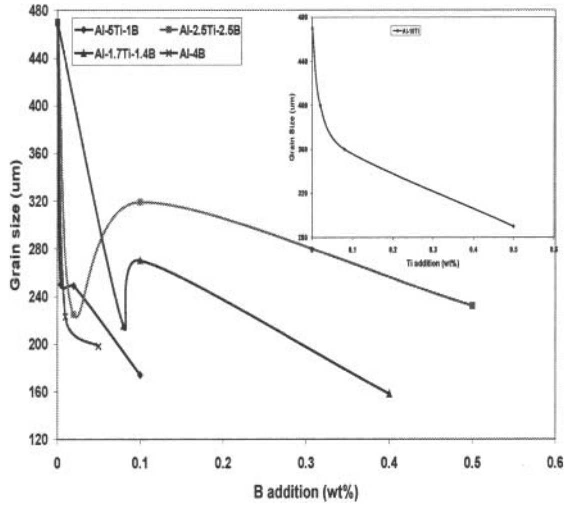

Figure 3. Average grain size of Sr-modified A356.2 alloy as a function of B addition levels using different grain refiners. Corresponding data for Ti additions using Al-10%Ti are also shown (inserted individual curve).

Figures 4(a) to (d) show the corresponding microstructures for low addition levels of Al-Ti-B in the form of master alloys combined with 200 ppm Sr. Figures 4(a) and (b) depict that no major change in the morphology of the Si particles; in this case, a boron-content of 0.004% and 0.016%, respectively, also becomes available in addition to the same content in Ti. With reference to Figure 4(c), grain refining was applied using the Al-2.5%Ti-2.5%B master alloy; the corresponding boron-content for this figure is 0.08%, while for Figure 4(d), where the Al-1.7%Ti-1.4%B master alloy was used, the boron-content is 0.066%. In Figure 4(c) some evidence of coarsening appears, while in Figure 4(d) the shape and size of the Si particles resemble those shown in Figure 4(b). It is clear that by gradually increasing the boron-content, a number of changes may occur in the shape and size of these particles; thus, for the Al-2.5%Ti-2.5%B master alloy, the addition of 0.08% Ti may be considered the threshold level for affecting silicon morphology by using boron. From a comparison of the microstructures shown in Figure 4, it may be concluded that there is no significant interaction between strontium and boron, or between strontium and titanium, at low addition levels of Ti and B.

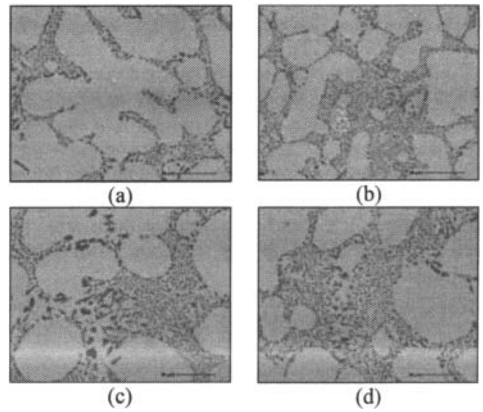

Figure 4. Optical micrographs showing the microstructures of as-cast 200 ppm Sr-modified A356.2 alloy after refining by addition of (a, b) 0.02% and 0.08% Ti, using Al-5%Ti -1%B; (c) 0.08% Ti, using Al-2.5%Ti -2.5%B; and (d) 0.08% Ti, using Al-1.7%Ti-1.4%B.

<u>Interaction of Grain Refiner and Modifier</u>

Figure 5 shows a backscattered image of an as-cast A356.2 alloy sample containing 0.5% Ti and 200 ppm Sr, and the corresponding EDX analysis of the particles observed in the image. The sample contains a number of tiny bright particles, approximately 1 μm or less in diameter which were originally believed to constitute a Sr-Ti compound, but this deduction has since been proven inaccurate. In order to determine the chemical composition of these particles, EDX and WDS analyses were conducted at 15 kV, but since the Kα line for Si is very close to the Lα line for Sr, no conclusions could be drawn with any certainty regarding the interaction between Ti and Sr.

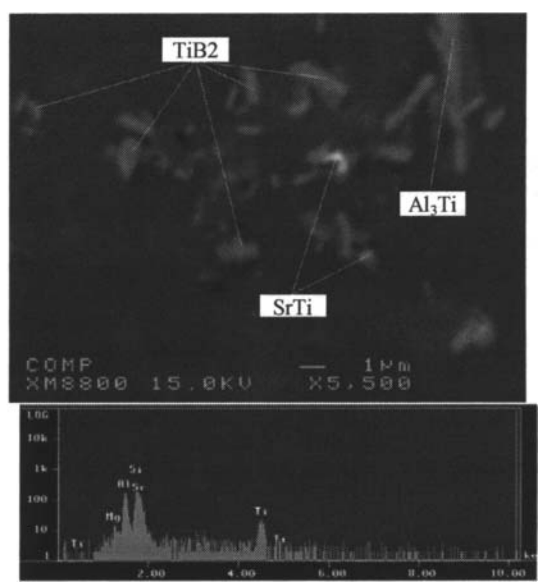

Figure 5. Backscattered image of different particle types observed in the alloy refined with 0.5% Ti using Al-5%Ti-1%B master alloy, and EDX spectrum.

Figure 6 shows the backscattered image and corresponding distribution of Sr and Ti in the as-cast 200 ppm Sr-modified A356.2 alloy sample containing 0.5% Ti added in the form of Al-10%Ti master alloy. In this figure, the backscattered image (a) and the X-ray image of Ti (b) show that the tiny bright particles do not contain Ti, *i.e.* the presence of these particles is not necessarily to be interpreted as evidence for a Ti-Sr interaction. The gap in the Sr element distribution map, as shown in Figure 6(c), clearly reveals that there is no diffusion between Ti and Sr atoms, or any tendency towards interaction between them.

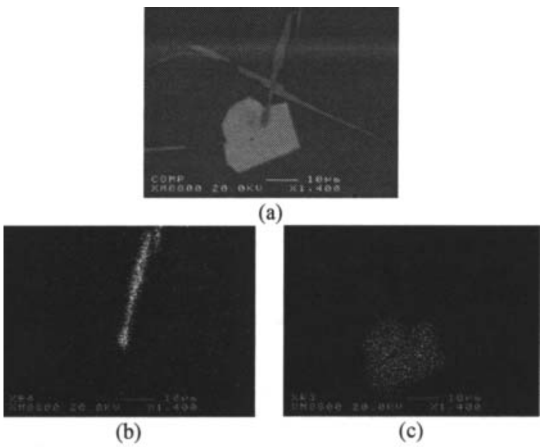

Figure 6. Proximity of Al_3Ti particle with Sr-rich particle in 200 ppm Sr-modified A356.2 alloy refined with addition of 0.5%Ti in the form of Al-10%Ti: (a) backscattered image; (b, c) X-ray images of Ti and Sr distribution, respectively.

Figures 7(a) to (d) illustrate the elemental distribution in the particles found in the as-cast sample of the 200 ppm Sr-modified A356.2 alloy, grain refined with 0.01% B added in the form of Al-4%B master alloy. A comparison of the X-ray images of Ti, B, and Sr suggests that, at low addition levels of B, there appears to be no given Sr potency which takes precedence over another for a reaction to take place with either Ti or B atoms.

Figure 8(a) shows a backscattered electron image of a cluster of AlB_{12} particles surrounded by a ring of TiB_2 particles; this configuration was observed with the addition of 0.05% B to the alloy using the Al-4%B master alloy. The corresponding X-ray images for B, Sr, and Ti are provided in Figures 8(b), (c), and (d), respectively. These images are presented as evidence for the greater tendency of B to react with Sr to form a Sr-B compound, as opposed to Ti. The fact that an AlB_{12} phase may be observed is, in all likelihood, the result of the excessive amount of Al-4%B master alloy (0.05% B) present in the melt, which would tend to explain why part of this phase remains unreacted. The composition of the intermetallic compounds shown in Figure 8(a) were analyzed using WDS and the average compositions are listed in Table 2. An increase in the Sr-content of the alloy would thus eventually lead to the formation of the non-heat-treatable intermetallic compound Al_4SrSi_2 which causes alloy embrittlement. Electron probe microanalysis of the particles observed showed that the composition of several of them is close to Al_4SrSi_2.

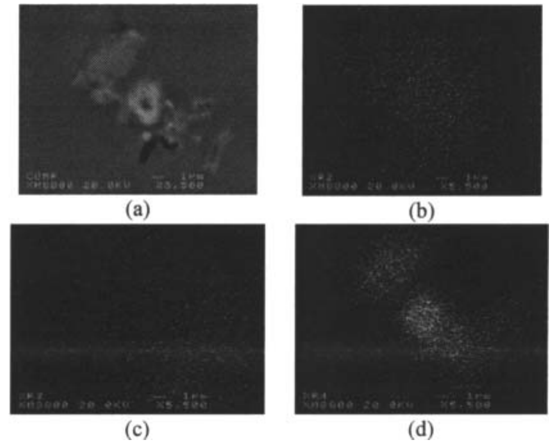

Figure 7(a) Backscattered electron image showing intermetallic particles found in 200 ppm Sr-modified as-cast A356.2 alloy refined by addition of 0.01% B using Al-4%B, and corresponding X-ray images of (b) B, (c) Sr, and (d) Ti.

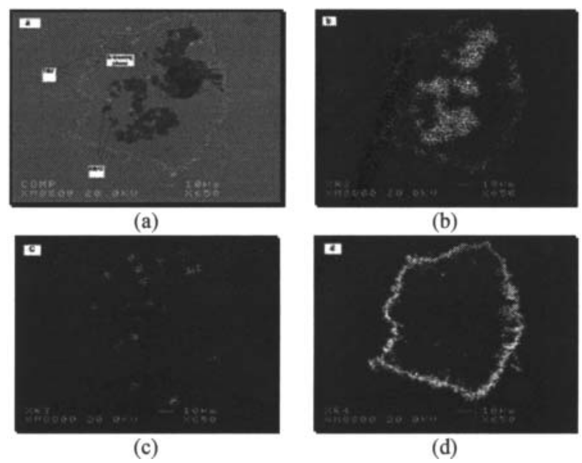

Figure 8(a) Backscattered electron image showing intermetallic particles found in 200 ppm Sr-modified as-cast A356.2 alloy refined by addition of 0.05% B using Al-4%B, and corresponding X-ray images of (b) B, (c) Sr, and (d) Ti.

Table 2. Average chemical composition of particles observed in as-cast A356.2 alloy refined with 0.05% B using Al-4%B.

Elements Present	Average (wt %)	Average (at.%)	Calculated Formula	Suggested Formula
Si	23.73	25.34		
B	4.24	12.42		
Ti	0.68	0.40	$Al_{4.5}SrSi_{2.4}$	Al_4SrSi_2
Al	40.74	46.92	+	+
Sr	27.73	10.38	B	B
Mg	0.90	1.08		
Total	98.02	96.54		
B	81.06	92.19		
Al	17.06	7.78	$AlB_{11.85}$	AlB_{12}
Total	98.16	99.97		

Figure 9 displays the X-ray mapping of a 200 ppm as-cast Sr-modified alloy refined with the addition of 0.5% B using Al-4%B. Figure 9(c) includes some bright particles with a broad size-range, where the corresponding WDS image confirms that these are Sr-rich particles. The proximity of the B-rich zones to the Sr-rich zones, and the fact that these elements co-exist in bright-particle locations, suggest that the particles contain, predominantly, B and Sr. The WDS analysis results shown in Table 3 suggest further that the composition of these particles is very close to the stoichiometric value of SrB_6. This observation indicates that certain portions of the boron tend to combine with Sr, instead of with Ti.

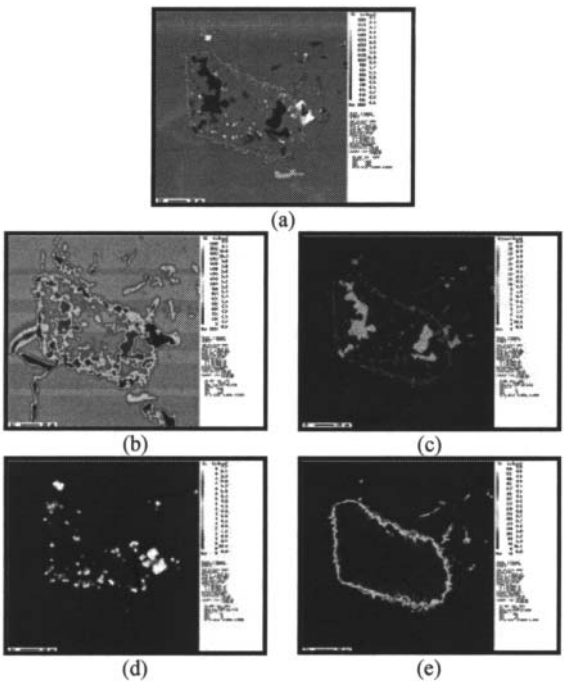

Figure 9(a) Backscattered image of a region which includes Sr-rich particles in as-cast Sr-modified A356.2 alloy refined with 0.5% B using Al-4%B and the corresponding X-ray images of (b) Al, (c) B, (d) Sr, and (e) Ti, respectively.

Table 3 Chemical composition of particles observed in Figure 9(a) as obtained from WDS analysis.

Elements Present	Average (wt%)	Average (at.%)	Calculated Formula	Suggested Formula
B Al Sr Total	48.32 0.12 55.82 103.26	87.35 0.09 12.46 99.90	SrB_7	SrB_6

The formation of SrB_6 compound consumes a large amount of Sr and B in the melts simultaneously, resulting in the reduction of freely available Sr and B for modification or refinement, respectively. These SrB_6 particles are relatively high in density [2], with a theoretical density of 3.422 g/cm^3, and they are therefore expected to precipitate gradually in the melt. As a result, a Sr and B rich intermetallic compound is expected to accumulate in the bottom layer of the melt, while the concentration of solute Sr in the melt decreases to a significant extent.

Thermal Analysis

In order to evaluate interactions between Sr and B, as well as between Sr and Ti, a number of thermal analysis experiments were conducted for this study. Both the influence of boron on strontium fading and the effect of the Sr-B interaction on the eutectic Si in the Sr-modified A356.2 alloy were investigated using the master alloy Al-4%B; whereas Al-10%Ti was used to examine Ti for the same purpose. Figure 10 illustrates that, within the range of 0.05 to 0.5% Ti used in this study, the eutectic temperature drops as Ti increases in comparison with the non-grain-refined 200 ppm Sr modified alloy, with a minimum at 0.3% Ti. The eutectic temperature thus shows signs of being affected by this range of Ti addition, implying that the presence of Ti in the melt promotes the modification of Si in this alloy.

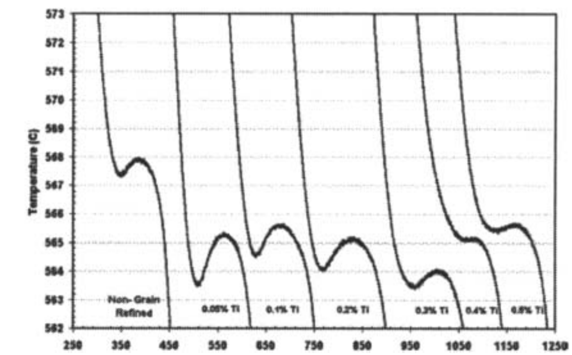

Figure 10. Cooling curves for thermal analysis of 200 ppm Sr-modified A356.2 alloy with different Ti additions using Al-10%Ti.

Figure 11 shows a corresponding set of cooling curves for additions of boron ranging from 0.05% to 0.5%. This figure shows two distinct regions: one in which the eutectic temperature decreases when the boron addition is less than approximately 0.2% B; and the other in which the eutectic temperature increases rapidly, rising even beyond the original temperature when B addition increases from approximately 0.2 to 0.5% B. It will be observed, therefore, that when the B increases, the eutectic growth temperature drops initially by almost 2°C until a 0.1% B level is attained, but when the boron is increased to higher levels, the eutectic growth temperature also increases. This behavior indicates that the interaction of Sr with B affects the modification of Si in A356.2 alloys, on condition that the amount of boron is higher than 0.1%.

A comparison between addition levels of B and Si modification shows that, in general, as the boron is increased to 0.1%, the degree of Si modification also increases. It is clear that the boron-content should not exceed 0.1% for Sr to modify the morphology of eutectic Si in the presence of a grain refiner. It may be also observed that the addition of boron has a slightly modifying effect on A356.2 alloys at low levels of addition.

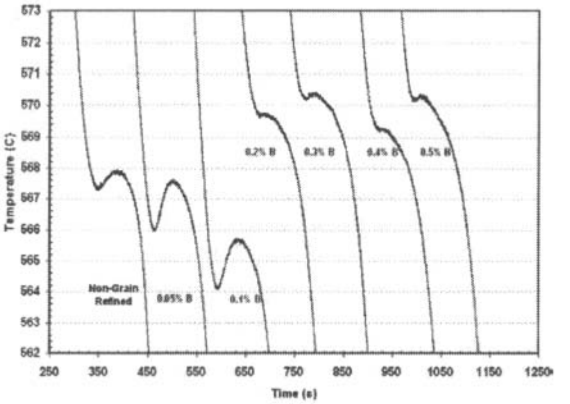

Figure 11. Cooling curves obtained from thermal analysis of 200 ppm Sr-modified A356.2 alloy with different B additions using Al-4%B.

Conclusions

Based on the results obtained from this research, the following conclusions may be drawn.

1. No sign of any Sr-Ti interaction was found over the range of Ti levels studied. This was confirmed by thermal analysis and electron probe microanalysis. Therefore, Ti addition does not have any adverse effect on the performance of Sr as a modifier in A356.2 alloy.
2. There is no significant Sr-B interaction at low addition levels of the Al-Ti-B type grain refiners up to 0.1% B. Increase in the B-content beyond this level leads to changes in the shape and size of the eutectic Si particles, as was observed in the microstructures of A356.2 alloy grain refined using Al-2.5%Ti-2.5%B and Al-1.7%Ti-1.4%B master alloys at B levels exceeding 0.1%. Thus, 0.1% B addition can be considered as the starting point for the eutectic Si particles to revert to coarse flakes in such cases.
3. A quantity of Sr-rich particles appear in the case of the alloy which had been refined with the addition of 0.5% B in the form of Al-4%B, after it was modified with 200 ppm of Sr; this would suggest that such particles contain B and Sr predominantly, with a composition approaching SrB_6.
4. The interaction between Sr and B may also lead to a decrease in the amount of boron available for TiB_2 formation and, hence, result in poor grain refining.

Acknowledgements

The authors would like to express their grateful acknowledgement for financial and in-kind support received from the National Sciences and Engineering Research Council of Canada; and from GM Powertrain Group.

References

1. Warmuzek M., *Aluminum-Silicon Casting Alloys, Atlas of Microfractographs* (ASM International, OH: Materials Park 2004).
2. S. Shivkumar, L. Wang, and D. Apelian, "Molten Metal processing of Advanced Cast Aluminum Alloys," *Journal of Metals*, Jan (1991), 26-32.
3. B. Closset and J.E Gruzleski, "Structure and Properties of Hypoeutectic Al-Si-Mg Alloys Modified with Pure Strontium," *Metallurgical and Materials Transactions A*, 3 (1982), 945-951.
4. D.G. McCartney, "Grain Refining of Aluminum and Its Alloys Using Inoculants," *International Materials Reviews*, 34 (5) (1989), 247-260.
5. M. Johnsson, L. Bäckerud, and G.K. Sigworth, "Study of the Mechanism of Grain-refinement of Aluminum after Additions of Ti-containing and B-containing Master Alloys," *Metallurgical Transactions A*, 24 (1993) 481-491.
6. M.M. Guzowski, G.K. Sigworth, and D.A. Sentner, "The role of boron in the grain refinement of aluminum with titanium," *Metallurgical and Materials Transactions A*, 18 (1987) 603-619.
7. S.G. Shabestari, and H. Moemeni, "Effect of Copper and Solidification Conditions on the Microstructure and Mechanical Properties of Al-Si-Mg Alloys," *Journal of Materials Processing Technology*, 147 (2004), 153-154.
8. G.K. Sigworth, M.M. Guzowski, "Grain Refining of Hypoeutectic Al-Si Casting Alloys," *AFS Transactions*, 1985, no. 92:907-912.
9. M. Johnsson, "A Critical Survey of the Grain Refining Mechanisms of Aluminum," *Chemical Communications*, 5 (1993), 33-40.
10. Y.C. Lee et al., "The Effect of Grain Refinement and Silicon Content on Grain Formation in Hypoeutectic Al–Si Alloys," *Materials Science and Engineering A*, 259 (1999), 43-52.
11. K. Kashyap, and T. Chandrashekar, "Effects and Mechanisms of Grain Refinement in Aluminium Alloys," *Bulletin of Materials Science*, 24(4) (2001), 345-353.
12. H. Liao, and Y. Sun, "Correlation between mechanical properties and amount of dendritic α-Al phase in as-cast near-eutectic Al-11.6% Si alloys modified with strontium," *Journal of Materials Science*, 37 (2002), 3489-3495.
13. H. Liao, and G. Sun, "Mutual poisoning effect between Sr and B in Al-Si casting alloys," *Scripta Materialia*, 48 (2003), 1035-1039.